Mercury, arsenic, lead and cadmium in waters of the Singrauli coal mining and power plants industrial zone, Central East India

Shefali Bhardwaj · Richa Soni · Sharad Kumar
Gupta · Dericks P. Shukla (iD)

Abstract The present investigation is an attempt to assess the contamination of heavy metals in the ground and surface water of the Singrauli industrial belt area. Pollution indices like heavy metal index (HPI), contamination index (CD) and heavy metal evaluation index (HEI) are used for the evaluation of heavy metal pollution (arsenic As, mercury Hg, cadmium Cd, and lead Pb). Contour maps are constructed to interpret metal spatial distribution. Further, the land-use/land-cover (LULC) maps for the year 2000, 2010 and 2016 are prepared using Landsat satellite data. A total of 48 water samples (Groundwater (27), Surface water (21)) are analysed for heavy metal concentration. Eighty-eight percent of groundwater and 90% of surface water samples are contaminated with Hg. Similarly, high concentrations of Pb and Cd were found in the samples. Surprisingly, all the water samples have As concentration above the WHO permissible limit of 10 ppb. Further, 95% of the samples have an HPI value greater than 100 indicating high heavy metal contamination. CD value denotes contamination of 89% of the samples with heavy metals (As, Hg, Cd, Pb). Through spatial distribution, it can be interpreted that most of the contaminated samples lie near thermal power plants, ash ponds, and coal mines. LULC (land use/land cover) study shows a significant decrease in water bodies by (108 km^2), agricultural land by (54 km^2) and bare/fallow land by (51 km^2) from 2000 to 2016. During these 16 years, there has been a fourfold increase in the overburden, a threefold increase in dumping yards, a 2.5 times increase in urban areas, and a twofold increase in mining areas. Both the environment and the water quality are deteriorating at an alarming rate. Such scientific investigations are relevant for risk management studies of potable water. The knowledge acquired from such assessment shall be considered with utmost priority by concerned authority considering degrading water quality in the study area. Hence, this study is applicable for designing action plans and control measures to reduce water resource pollution.

Introduction

Balancing the supply of freshwater with increasing demands is a major global challenge for the growing populations of the world. The exponential growth of population in various regions in recent decades has led to enhanced urbanization and rapid industrial growth, which in turn led to the exploitation of water resources (Simeonov et al. 2003; Brindha et al. 2014). The quality of water is deteriorating globally; hence, water pollution

S. Bhardwaj · R. Soni · S. K. Gupta · D. P. Shukla (✉)
School of Engineering, Indian Institute of Technology Mandi,
Room No. 301, A-4 Building, IIT Mandi, South Campus,
Kamand, Mandi, Himachal Pradesh 175005, India
e-mail: dericks@iitmandi.ac.in

e-mail: dericks.82@gmail.com

is emerging as a major concern for the twenty-first century. Water gets contaminated either by natural processes or through anthropogenic activities. Example of natural processes are leaching of minerals, interaction of rocks with water, groundwater movement and mineralisation (Shukla et al. 2010, Machiwal and Jha 2014, Raju et al. 2009); while anthropogenic activities include discharge of domestic sewage, industrial discharge (slurry water and drain water), agricultural runoff and mining activities (Simeonov et al. 2003; Singh et al. 2005; Sharma et al. 2007; Förstner and Wittmann 2012). About two million tons of waste (sewage, industrial, agriculture) is discharged into world water daily (UN WWAP 2003).

Pollution of water resources with heavy metals like mercury, arsenic, lead, cadmium, iron, and zinc has become a concern in the Indian sub-continent. Many parts of India such as the western part of Uttar Pradesh (UP), Jharkhand, West Bengal, Punjab and Orissa are facing scarcity of potable water (Tiwari et al. 2014). Ninety percent of urban and 20% of the rural Indian population are dependent on untreated ground and surface water resources. More than ten million Indians are at risk of fluoride and arsenic contamination as they are over-dependent on groundwater resources (Singh et al. 2007). According to one report, the Ganga-Meghna-Brahmaputra region is widely contaminated with heavy metal Arsenic (Chakraborti et al. 2013). More than 30 districts in UP have arsenic concentrations above the WHO permissible limit of 10 ppb (WHO 2011) in groundwater (Yano et al. 2012). The origin of these contaminants can be either natural or anthropogenic depending on variations in different geo-environmental settings. However, the main anthropogenic contributors of heavy metal pollution in water resources are industrial discharges, mining activities, coal-based thermal power plants, use of arsenic-based fertilizers, and agriculture runoff (Sharma et al. 2007; Pandey et al. 2011; Dubey et al. 2012; Chowdhury et al. 2016; Singh and Kumar 2017; Usham et al. 2018).

As India is blessed with a rich variety of mineral resources, mining is a key industry of the country (Mehta 2002). The major mineral resource is coal, which is being mined extensively. It is the primary fuel for power generation in India accounting for 50–55% of the total power generation. However, coal mining has adverse consequences on the environment such as soil erosion, acid mine drainage, agricultural land degradation and changes in natural topography and drainage pattern. Runoff water from coal washeries can further contaminate ground and surface water as they carry loads of heavy metal (Finkelman 2007). The combustion of coal in thermal power plants (TPP) is concluded to be a major source for water pollution (Dubey et al. 2012,). The combustion of coal, mostly in thermal power plants (TPP), generates huge amounts of the bottom and fly ash. This ash is mainly discarded in ash ponds near some water sources such as a river or a lake (reservoir) while only 5% is utilized in various processes (Bhattacharjee et al. 2002). Ash contains many harmful heavy metals and has the potential to contaminate both ground and surface water resources. Hence, both the production and the combustion of coal contribute to the release of harmful heavy metals in the surrounding through different pathways.

An area where there are many open cast coal mines and TPPs is the Singrauli region in central India which has been declared a critically polluted region by the Ministry of Environment and Forests (MoEF). This region is one of the most highly polluted industrial areas of Asia and it has an extremely high comprehensive environmental pollution index (CEPI) of CPCB (Sahu et al. 2014). Owing to the presence of many TPPs, this region is recognized as "Energy Capital" of India. These TPPs are considered as the main source of pollution in this region contaminating the river, ground and reservoir (Rihand reservoir) water (Pandey et al. 2011). Even the soil samples that are collected from various sites near the mining area indicate a higher concentration of Cd, Pb, As and Ni (Agrawal et al. 2010). A study carried out by the Centre for Science and Environment (CSE) found significant concentrations of heavy metals such as mercury in people residing in this area (CSE 2011). In addition, the air quality of this region is very poor and the primary reason of atmospheric pollution is the emission from these coal-based TPPs (Prasad et al. 2012).

The emission from these coal power plants is the source of conditions like dust, haze and smog in this region. Annually, six million tons of fly ash is emitted from these TPPs. In some parts of Singrauli area, this fly ash lies in 5-ft. thick piles, which has toxic heavy metals like mercury, cadmium, lead and arsenic in addition to fine particles (Yadav et al. 2017). The most common illness that is witnessed in this region is tuberculosis, bronchitis and asthma, which are associated with the inhalation of fine dust particles and fly ash fines (Yadav et al. 2017). Due to the incomplete combustion, these TPPs result in the emission of black carbon (BC) soot

that can affect both human health and vegetation. The very high concentration of BC (> 200 $\mu g/m^3$) and aerosol optical depth (AOD) (~ 1.0) is observed near thermal power plants in Singrauli area (Singh et al. 2018).

However, heavy metal contamination study in various water bodies such as ground, pond, reservoir and drain water has not been carried out extensively. Hence, this study attempts to assess the variations of heavy metal in groundwater (hand pump) and surface water (drain, pond and dam reservoir water) with the spatial distribution of heavy metals such as arsenic and mercury and thus figure out the impact of coal mining. Various pollution indices such as heavy metal pollution index (HPI), heavy metal evaluation index (HEI) and contamination index (CD) are used for the evaluation of water pollution in the study area. Finally, the changes in land use/land cover of this industrial belt have been assessed with the help of remote sensing and geographical information systems (GIS) to evaluate the impact of coal mining and waste dump from these TPPs.

Material and methods

Study area

As mentioned earlier, the Singrauli region is designated as a critically polluted area (CPA) by MoEF. This region is located between 24°03′N to 24°33′N latitude and 82°33′E to 83°03′E longitude sharing the border of Singrauli district of Madhya Pradesh and Sonebhadra district of Uttar Pradesh. Figure 1 shows the location of various samples near the Rihand dam reservoir. These samples have been taken from the vicinity of Renukoot, Anpara, Vindhya Nagar, Kakri Mines, Khadia Mines and Jayant Mines. The satellite image of 2016 is taken by using NIR, RED AND GREEN bands. The study area covers an area of approximately 3020 sq. km. The development started in this area after the construction of the Rihand dam in 1962 (Govind Ballabh Pant Sagar dam) on River Rihand which is a tributary of Sone River. With the discovery of abundant coal reserves in the western part of Rihand Dam, the exploitation of the area began in the form of open cast mines. Due to the presence of various coal mines and abundant water supply from the Rihand dam reservoir, many thermal power plants (TPPs) and industries were established in this area (Khan et al. 2013). These industries and various mining operations in the region are considered to be the

potential sources for contamination of water, air and soil, thus, affecting the health of the people staying here.

Geologically, the study area falls in the Vindhyan (Kaimur and Semri Groups) and Gondwana Supergroups which comprises mainly of sedimentary rocks such as sandstone, limestone, quartzitic sandstone, and quartzite; Precambrian Mahakaushal Group comprising of volcano sedimentary rock formations; and Precambrian Chotanagpur Granitic-Gneiss Complex comprising predominantly of migmatitic granitic gneisses and porphyritic granites (Kumar and Ahmad 2007; Singh and Srivastava 2011; Usham et al. 2018). The granitic-gneissic complex is situated in the eastern side of the study area while the western side is mainly composed of Gondwana Supergroup. This Permo-Carboniferous Supergroup hosts coal bearing formations of Barakar, Talchir and Raniganj formations. Most of the coal mines of the study area extract coal from Gondwana Supergroup (Singh et al. 2014; Usham et al. 2018). The depth of the dug wells ranges from 3 to 21 mbgl with depth to water level varies from 2.41 to 16.70 mbgl. In the pre-monsoon season, the water level raged from 8 to 12 bgl in the district while in post monsoon it ranges from 5 to 10 bgl (CGWB 2013).

Water sampling

Extensive field work was carried out in this region in December 2015. More than 50 water samples in duplicate were collected from this region. Out of these samples, 27 samples were collected from the groundwater, mainly hand pumps in the vicinity of the human settlements. Twenty-one samples of surface water were collected from various ponds, drains including slurry water and reservoir water. The water in the ponds is mainly used for washing purposes and irrigation in the agriculture field. The drains from the power plants pass their effluents and waste to Rihand dam reservoir water. Two spare samples of ash slurry water from ash-pond were collected for future studies. As most of the mines and coal-based TPPs are located on the western side of the reservoir, sampling was carried out on this site only. Samples were collected in duplicate in 1-L polypropylene sample collection bottles. These sample collection bottles were soaked in 10% HNO_3 for 24 h and properly dried before taking to field work. The sampling bottles were rinsed many times with the same water and then completely filled till the brim and tightly closed to minimize any contact with air (Shukla et al. 2010).
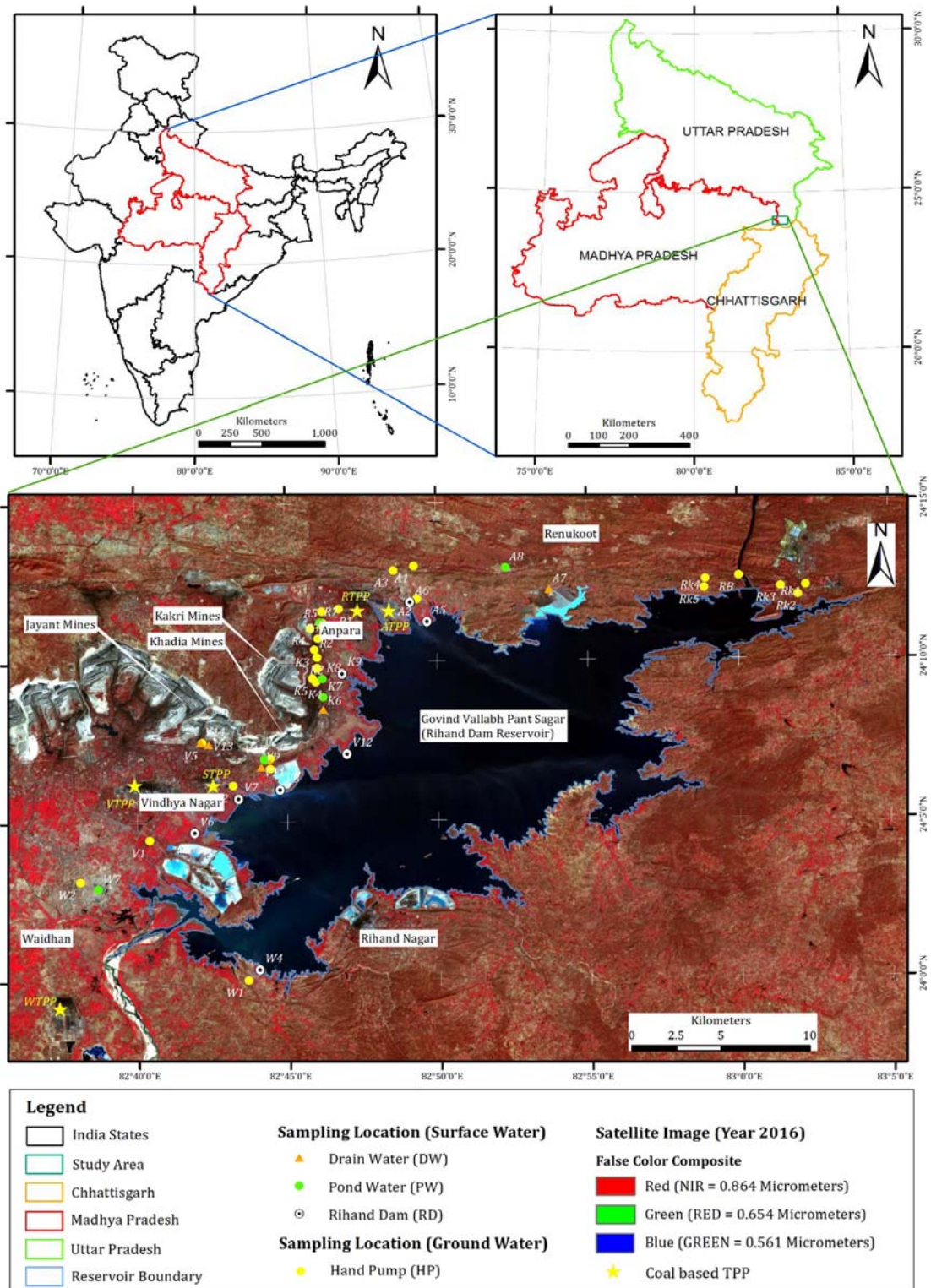
Fig. 1 Study area map showing sampling locations in the vicinity of coal mines, TPPs, and Rihand reservoir. Five TPPs in the study area are ATPP: Anpara Thermal Power Plant; RTPP: Renusagar Thermal Power Plant; STPP: Shaktinagar Thermal Power Plant; VTPP: Vindhyachal Thermal Power Plant; WTPP: Waidhan Thermal Power Plant. The areal extent is shown by Landsat satellite image of 2016 displayed using standard false colour composite (FCC)

Physical parameters like pH and temperature are measured on the field using digital instrument. The water samples were filtered using 0.45-µm filter paper and preserved by adding concentrated nitric acid (HNO_3) (2 ml) to maintain the pH of 2, and were brought to the laboratory at Indian Institute Technology (IIT) Mandi. One set of the samples were sent to NABET (National Accreditation Board for Education and Training) accredited laboratory i.e. CEG Test House, Malviya Nagar in Jaipur for heavy metal analysis: mainly As, Hg, Cd and Pb, using ICPMS and one set of samples were analysed at IIT Mandi using Heavy Metalyser HM 1000 (Soni and Shukla 2018). The flowchart for the methodology adopted in our study is shown in Fig. 2.

Analytical work (heavy metal analysis with Metalyser HM 1000)

The Metalyser HM 1000 has a lower limit detection of 10, 3, 5 and 5 ppb for As, Cd, Hg and Pb, respectively, and the upper limit is 500 ppb for all the four heavy metals. This instrument has a correlation of 97% for estimation of As with graphite furnace atomic absorption spectrometry (GF-AAS) Swash (2003). In addition, it is certified by the Sri Ram Institute, Delhi and University of Delhi (Shukla et al. 2010; Dubey et al. 2012). Such hand-held instruments are useful for As testing (up to 100 ppb) in the field having a correlation of 0.95 with laboratory measurements (Sankararamakrishnan et al. 2008).

The operating procedure of metalyser is voltammetry method that consists of two main steps—conditioning and analysis. It is essential that a working electrode is conditioned and plated first for the metal of interest before any analysis. For ease of access, the metals are clubbed and renamed into M groups with different numbers. Cd and Pb fall under M1 group while Hg and As fall under M2 and M3 group, respectively. For each analysis, the same M group number is used for all the buffers, conditioning reagent and standards. Several samples can be analysed for the metals once the conditioning and calibration step is complete. The first step in conditioning involves the use of either M1 or M2 or M3 (depending on the element to be assessed) conditioning solution that forms a thin coating plate on the working electrode. After proper conditioning, the grey colour coating is seen on the electrode for Cd and Pb analysis; yellow colour coating should be

visible prior to the analysis of As and Hg. Second layer of conditioning is also carried out to achieve the reliable results.

Further, the analysis is done via a calibration method that establishes a calibration curve first before analysing a number of samples rapidly. The calibration needs to be established just prior to analysis and also after a new plate is formed on the tip of the working electrode. After successful conditioning, the respective metal buffer is added to sample beaker, for example, M1 a & b buffer for the analysis of Cd/Pb while M2 and M3 for Hg and As analysis, respectively. 20 ppb (280 µl) of respective metal standards M1/M2/M3 is added. 20 ppb standard is added twice at an interval of 2 min to get three-point calibration curve of 20, 40 and 60 ppb. After the calibration, several successive analyses were carried out for respective heavy metals in the water samples. For analysis of Cd and Pb, 70 ml of water sample was taken and M1&4a and M1&4b buffer sachets were added to the sample beaker. Similarly, M2 buffer sachets is added in 70 ml water sample for Hg analysis. For total arsenic analysis, 67 ml of the water sample is added with 3 ml of 12 M concentrated HCL. The acid functions as the oxidizing agent and buffer. Then the conditioned electrode is dipped in the water sample and based on the calibration curve (already stored in its memory) the concentration of the sample is measured.

Spatial distribution analysis

The data points for the contaminants were divided as either ground or surface water and plotted in a GIS environment using ArcGIS 10.3 software. These data points were interpolated to obtain the spatial distribution of respective contaminants in the study area to ascertain the anthropogenic effects. Inverse Distance Weight (IDW) technique is used for interpolation considering that as one moves away from the observed data point, its concentration will decrease.

Pollution evaluation indices

In this study, we are using heavy metal pollution index (HPI), heavy metal evaluation index (HEI) and contamination index (CD). The hand pump water is taken as groundwater and surface water is divided into three
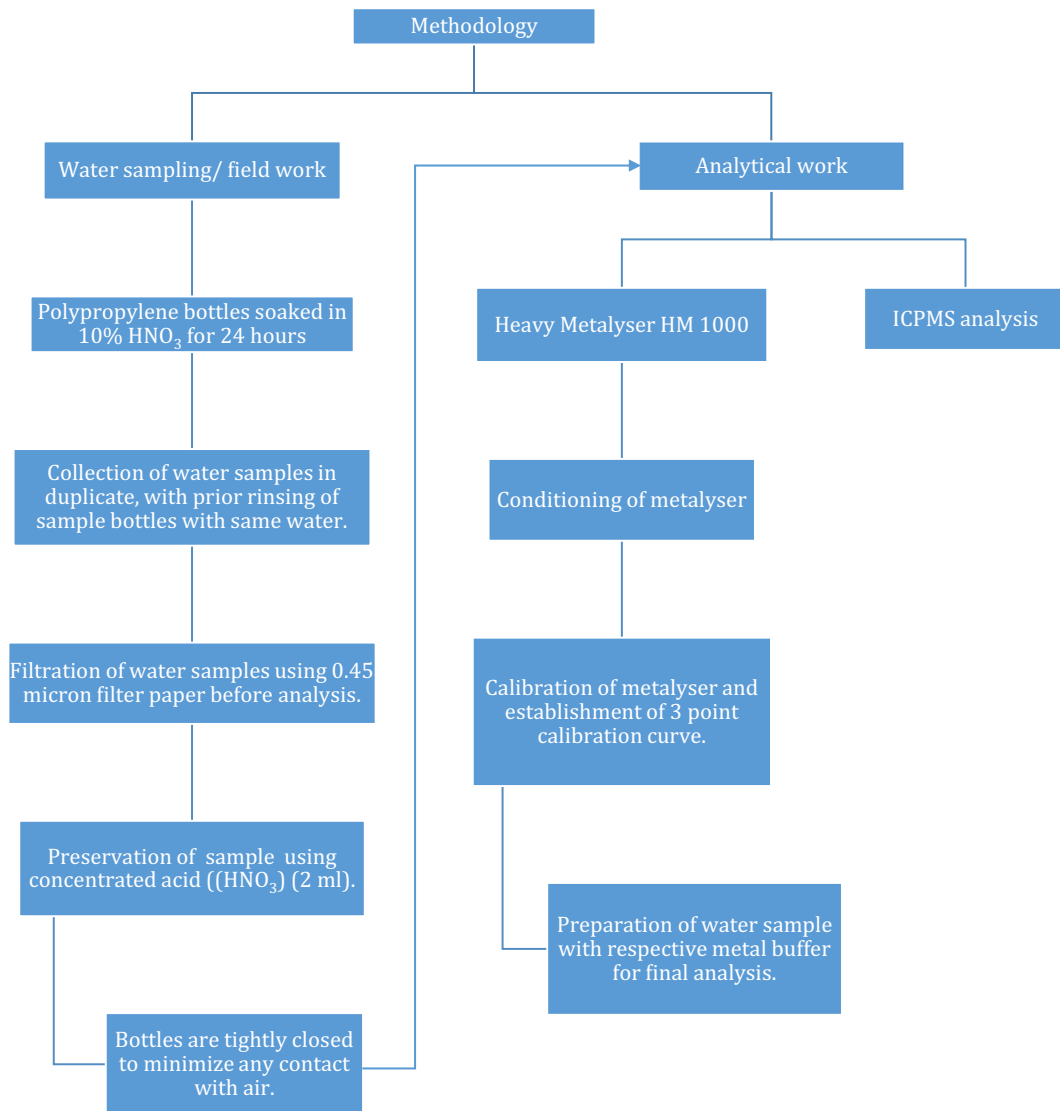
Fig. 2 Flowchart showing the methodology followed during sampling and analysis

categories (drain water, pond water and reservoir dam water). Details about these indices are given below.

Heavy metal pollution index (HPI)

The combined effects of each heavy metal on the overall quality of water can be evaluated using heavy metal pollution index (Tiwari et al. 2014). Two steps are involved in its calculation. Firstly, a rating scale is prepared for selected parameters and secondly, a pollution parameter is selected based on which index is formed (Giri and Singh 2014). For HPI, a unit weightage (W_i) is calculated that is inversely proportional to the recommended standard (S_i) of the corresponding parameter (Giri and Singh 2014). Here, we are using Bureau of Indian Standard drinking water thresholds (BIS 2012) for calculating W_i. After that, a quality rating (Q_i) is prepared and the summation of these subindices in the overall index gives the HPI as mentioned in the formula (Prasad and Bose 2001).

$$HPI = \frac{\sum_{i=1}^{n} W_i Q_i}{\sum_{i=1}^{n} W_i}$$

The sub-index (Q_i) of the parameter is calculated by

$$Q_i = \sum_{i=1}^{n} \frac{(M_i(-)I_i)}{(S_I - I_i)}.$$

S_i = highest permissible limit; I_i = maximum desirable limit; M_i = monitored value of ith parameter. The (−) sign means only the difference value is kept and the sign is neglected. Both the value for S_i and I_i were taken from BIS 2012. The value of S_i is taken as 50, 1, 10 and 3 ppb for As, Hg, Pb and CD, respectively. The maximum desirable limit for As, Hg, Pb and Cd is taken as 10, 0, 0 and 0, respectively (BIS 2012).

Heavy metal evaluation index (HEI)

Heavy metal evaluation index is a method through which water quality can be estimated with respect to heavy metals. HEI is calculated as given by Edet and Offiong 2002.

$$HEI = \sum_{i=1}^{n} \frac{H_c}{H_{mac}}$$

H_c = monitored value; H_{mac} = maximum admissible concentration (mac) of ith parameter.

Contamination index

Another method for evaluating the quality of water is contamination index (CD) that summarizes the degree of contamination of different parameters that are harmful to domestic water (Backman et al. 1997). For its calculation, the contamination factor is calculated for each individual parameter and then its summation gives the value of contamination index. Different values of contamination index are found in different locations considering only four contaminants i.e. As, Hg, Pb and Cd. It is calculated as follows

$$C_d = \sum_{i=1}^{n} C_{fi}$$
$$C_{fi} = \frac{C_{Ai}}{C_{Ni}} - 1$$

C_{fi} = contamination factor of ith component; C_{Ai} = analytical value of ith component; C_{Ni} = upper permissible concentration of ith component. Edet and Offiong (2002) had taken the value of MAC (maximum admissible concentration) for C_{Ni}. However, after December 2003, MAC was abolished and "parametric valve" is defined as per European Union Council directive 98/83/

EC. Hence, in this study, limiting values of 50, 1, 10 and 3 ppb for As, Hg, Pb and Cd, respectively, are used as upper permissible concentration (C_{Ni}).

Land use/land cover (LULC) studies

Land use and land cover are two different terms that are frequently used together (Dimyati et al. 1996). The former refers to the functional employment of the land while the latter depicts the characteristics of the earth's surface in physical terms (Rawat and Kumar 2015). The areal increase in mining and other LULC classes is assessed through remote sensing and Geographical Information Systems (GIS) environment using ENVI 5.3 and ArcGIS 10.3 software.

LULC changes for the study area were carried out for different years using multi-temporal satellite data of 2000, 2010 and 2016. Landsat 7, Landsat 5 and Landsat-8 satellite images at 30 m spatial resolution are used for 2000, 2010 and 2016 years, respectively. Visual image interpretation technique is used for the selection of training sites which were used for image classification using Support Vector Machine (SVM) algorithm. LULC map was prepared for 11 classes that are industry, agriculture, vegetation, water body, ash pond, ash water, mine area, dumping yard, overburden area, urban area and bare land. The areal variation in each LULC class for different years is computed in ArcGIS 10.3 to analyse the change in spatial distribution area statistics.

Results and discussions

The concentration of various heavy metals (As, Hg, Pb and Cd) in the groundwater and surface water samples is presented in Table 1. Various pollution indices were also calculated as explained in earlier sections and are given in Table 1. The statistical summary of the samples is provided in Table 2. The permissible limit of groundwater is considered from WHO 2011. As surface water samples in this study comprises of Rihand Dam reservoir water, pond water and drain water samples, so for evaluating the water quality, we considered the limit defined by Environmental Protection Act (EPA 2002) for effluent discharge. The drains coming out of power plants and the ponds are drained into reservoir, thus, we considered it as effluent water. However, the Rihand dam water cannot be considered as effluent water, but

we took the conservative approach to analyse such surface water samples.

Heavy metal contamination (As, Hg, Pb, and Cd)

The arsenic (As) concentration in the water samples varied from nearly 12 to 209 ppb (Table 1). Considering the WHO permissible limit of 10 ppb of As in water; all the water samples have a concentration above this limit as shown in Fig. 3(a). Interestingly, the average and median concentration of As in groundwater are 78.87 ppb, 72.84 ppb while in surface water, it is 43.06 ppb, 31.00 ppb, respectively (Table 2). 9.52% of the surface water sample has As concentration above EPA guidelines of effluent discharge (EPA 2002). Therefore, the groundwater samples have a higher concentration of arsenic as compared to those of surface water. However, the highest concentration of 209 ppb is observed in one surface water sample (V9-drain water) which lies near Vindhyachal TPP. Two hand pumps i.e. K1 (near Kakri coal mine) and R3 (near Renusagar TPP-Parasi coal mine) area have high As concentration of 196 ppb and 198 ppb, respectively, which is nearly 20 times the WHO permissible limit (WHO 2011).

Mercury (Hg) concentration in the Singrauli Industrial area varies from nearly 5 to 33 ppb, though the WHO permissible limit is 1 ppb (Table 1). Except a few locations where no data value is observed, all locations have Hg concentration above the WHO limit. The average Hg concentration is nearly similar in both groundwater (10.81 ppb) and surface water (9.95 ppb). 52.38% of the surface water sample are exceeding EPA limit of Hg (5 ppb) as effluent discharge (Table 2). The median concentration in surface water (9.82 ppb) is similar to the average concentration, while that in ground water is 7.41 ppb. Thus, on average, the Hg concentration in water of this region is roughly ten times higher than the permissible WHO limit. The highest concentration of Hg (33 ppb) is observed in a hand pump location (R4) near Renusagar TPP-Parasi coal mine area (Fig. 3b). Similarly, high concentration (4.1 ppm) of Hg was observed in Rihand dam reservoir water (Rai 2008).

Lead (Pb) and Cadmium (Cd) concentration vary from nearly 5 to 317 ppb and 3 to 108 ppb, respectively (Table 1), in the study area. 88% of the ground water samples have Pb concentration higher than the WHO drinking water limit of 10 ppb. While 4.76% surface water sample have Pb concentration above EPA effluent discharge limit of 50 ppb. Further, the highest value

(317 ppb) observed at one location near Rihand Bridge. The areas near Anpara TPP and Renusagar TPP have also high concentrations of Pb with the highest being 225 ppb in a hand pump (A4) sample (Fig. 3c). The mean and median Pb concentrations in groundwater samples are 72.63 ppb and 22.55 ppb, respectively, while that of surface water is 35.72 ppb and 27.51 ppb (Table 2). Thus, the groundwater is more contaminated than surface water. Similar observations have also been reported by Agrawal et al. (2011) in the vicinity of Anpara TPP and Renusagar TPP. Also, high concentrations of Pb were observed in water samples of a well near Yatagan power plant, Mugla city, Turkey (Baba et al. 2003). Very high concentration of Pb (17 ppm) was observed at Belwadha site near Anpara power plant (Rai 2009).

Nearly 83% of the samples have Cd concentration beyond the WHO permissible limit of 3 ppb with the highest value (108 ppb) recorded in a hand pump (R2) near Renusagar TPP. The mean and median Cd concentrations in groundwater samples are 34.42 ppb and 7.48 ppb while that in surface water samples are 22.56 ppb and 23.98 ppb respectively. Thus, the mean concentration varies 7 to 11 times the WHO permissible limit. In comparison to groundwater, surface water is less contaminated (Fig. 3d). Still high values are recorded at various locations with the highest value of 40 ppb (A7) in the drain water of Anpara TPP. 14.28% of surface water samples are exceeding EPA effluent discharge limit of 10 ppb The high concentration of Cadmium was earlier reported in water samples near Anpara TPP and Renusagar TPP in Sonebhadra district of Uttar Pradesh (Agrawal et al. 2011). Similarly, very high concentration of Cd (4.5 ppm) was recorded at Belwadh site near Anpara TPP (Rai 2009).

The burning of coal is considered as the potential source for leaching of As, Hg, Pb and Cd into soil, surface water and groundwater (Fytianos et al. 1998; Kim and Kazonich 1999; Finkelman 2007; Agrawal et al. 2011, Sahoo et al. 2016; Das et al. 2018; Li et al. 2018). In one study involving contamination of groundwater in areas of Gonabad and Bajestan, Eastern Iran, 33% and 52% of the rural areas have Cd value above WHO limit of 3 ppb (Qasemi et al. 2019). In another study carried out to determine the heavy metals in groundwater of Lower Dir, Pakistan (Rashid et al. 2019) revealed the contamination Pb in 70% and Cd in 45% of the samples. High Pb and Cd concentrations are observed in various industrial areas of India such as

Table 1 Sample locations with corresponding heavy metal (As, Hg, Pb and Cd) concentration in ppb. HPI, CD and HEI computed using concentration of all these heavy metals are also given. Samples that were below detection limit (BDL) are marked as –

Sr. no	Location name	Code	pH	Type	Source	Arsenic (ppb)	Mercury (ppb)	Lead (ppb)	Cadmium (ppb)	HPI	CD	HEI
1	Anpara 1	A1	6.80	GW	HP	110	6	18	–	519.50	22.90	25.90
2	Anpara 2	A2	6.50	GW	HP	56	–	11	7	65.63	1.65	4.65
3	Anpara 3	A3	8.90	GW	HP	112	4	78	49	734.04	26.67	30.67
4	Anpara 4	A4	6.10	GW	HP	22	5	225	80	1083.74	50.13	54.13
5	Kakri 1	K1	6.10	GW	HP	196	13	127	94	1698.85	56.79	60.79
6	Kakri 2	K2	6.19	GW	HP	78	19	22	5	1376.02	20.69	24.69
7	Kakri 3	K3	6.40	GW	HP	26	8	16	6	606.06	8.04	12.04
8	Kakri 4	K4	6.40	GW	HP	23	5	15	4	354.16	3.89	7.89
9	Kakri 5	K5	6.40	GW	HP	30	8	–	–	560.76	6.73	8.73
10	Renukoot 1	Rk1	6.80	GW	HP	81	5	4	3	352.76	3.71	7.71
11	Renukoot 2	Rk2	6.60	GW	HP	57	29	156	108	2941.09	77.83	81.83
12	Renukoot 3	Rk3	6.70	GW	HP	45	4	12	6	358.57	4.59	8.59
13	Renukoot 4	Rk4	6.50	GW	HP	98	14	23	6	1030.55	16.36	20.36
14	Renukoot 5	Rk5	6.60	GW	HP	118	–	160	–	113.63	16.33	18.33
15	Renusagar 1	R1	6.70	GW	HP	73	–	–	–	2.16	0.46	1.46
16	Renusagar 2	R2	6.40	GW	HP	110	5	131	103	1243.84	50.90	54.90
17	Renusagar 3	R3	6.40	GW	HP	198	16	110	8	1240.60	29.47	33.47
18	Renusagar 4	R4	6.30	GW	HP	93	33	70	51	2738.83	55.17	59.17
19	Renusagar 5	R5	6.42	GW	HP	56	4	12	36	585.96	14.74	18.74
20	Rihand Bridge	RB	6.20	GW	HP	128	12	317	–	1072.40	43.58	46.58
21	Vindhya Nagar 1	V1	7.80	GW	HP	36	16	24	28	1347.65	24.75	28.75
22	Vindhya Nagar 2	V2	8.00	GW	HP	42	12	5	–	815.02	10.11	13.11
23	Vindhya Nagar 3	V3	7.60	GW	HP	34	6	16	3	457.21	5.36	9.36
24	Vindhya Nagar 4	V4	8.00	GW	HP	129	4	108	84	1012.29	41.58	45.58
25	Vindhya Nagar 5	V5	6.70	GW	HP	54	16	5	2	1094.69	13.90	17.90
26	Waidhan 1	W1	7.80	GW	HP	106	5	134	–	425.61	17.30	20.30
27	Waidhan 2	W2	7.60	GW	HP	17	7	18	5	518.33	6.53	10.53
28	Anpara 5	A5	7.30	SW	RD	19	10	–	–	702.82	8.58	10.58
29	Anpara 6	A6	7.10	SW	RD	39	7	–	–	460.65	5.47	7.47
30	Anpara 7	A7	6.50	SW	DW	136	14	30	40	1273.91	28.68	32.68
31	Anpara 8	A8	6.60	SW	PW	31	–	13	14	115.81	3.54	6.54
32	Kakri 6	K6	6.60	SW	DW	47	5	–	–	374.22	4.36	6.36
33	Kakri 7	K7	6.60	SW	PW	32	5	–	–	378.51	4.13	6.13
34	Kakri 8	K8	6.70	SW	PW	21	21	122	–	1547.37	30.91	33.91
35	Kakri 9	K9	6.80	SW	RD	12	4	28	34	578.26	14.72	18.72
36	Renusagar 6	R6	6.30	SW	DW	35	5	–	–	331.82	3.51	5.51
37	Renusagar 7	R7	6.60	SW	PW	33	–	8	3	27.03	0.60	2.40
38	Vindhya Nagar 10	V10	4.12	SW	PW	40	22	–	–	1514.79	20.80	22.80
39	Vindhya Nagar 11	V11	6.80	SW	DW	28	4	–	–	277.22	2.58	4.58
40	Vindhya Nagar 12	V12	8.10	SW	RD	24	4	–	–	303.22	2.87	4.87
41	Vindhya Nagar 13	V13	5.90	SW	DW	23	5	28	–	372.36	5.34	8.34
42	Vindhya Nagar 14	V14	6.71	SW	DW	21	5	–	–	344.42	3.42	5.42
43	Vindhya Nagar 6	V6	6.90	SW	RD	17	11	–	–	739.92	9.09	11.09

Table 1 (continued)

Sr. no	Location name	Code	pH	Type	Source	Arsenic (ppb)	Mercury (ppb)	Lead (ppb)	Cadmium (ppb)	HPI	CD	HEI
44	Vindhya Nagar 7	V7	5.90	SW	RD	14	11	–	–	743.94	9.09	11.09
45	Vindhya Nagar 8	V8	8.20	SW	RD	67	19	–	–	1317.55	18.45	20.45
46	Vindhya Nagar 9	V9	6.51	SW	DW	209	11	–	–	777.49	13.38	15.38
47	Waidhan 4	W4	7.30	SW	RD	18	10	21	–	690.42	9.29	12.29
48	Waidhan 7	W7	8.40	SW	PW	39	12	–	–	837.00	10.92	12.92

SW surface water, *GW* ground water, *HP* hand pump, *DW* drain water, *PW* pond water, *RD* Rihand Dam Water

Kanpur-Unnao having 86–895 ppb of Pb and 37–74 ppb of Cd (Dwivedi and Vankar 2014); Bangalore up to 170 ppb of Pb and 50 ppb of Cd (Gowda et al. 2003); Tuticorin in Tamil Nadu having 63–704 ppb of Pb and 9–49 ppb of Cd (Selvam et al. 2015). Lower concentrations of lead and cadmium are observed in the regions where mining and industrial activities are absent.

Spatial distribution of As and Hg in ground and surface water

The main objective of our study is to evaluate the metal pollution through indexing approach and interpretation of its source through spatial modelling. The heavy metals in the water resources cannot be fully monitored by classical monitoring methods and need spatial modelling plus GIS approach. Many studies have evaluated the spatial distribution and risk assessment of heavy metals in environment (Zhang et al. 2017; Lü et al. 2018; Torregroza-Espinosa et al. 2018; kalita et al. 2019). A study carried out to determine the spatial distribution of arsenic in groundwater of Bengal basin, India (Ghosh et al. 2019) interpreted the future trends of arsenic contamination. In another study, using integrated geostatistical models revealed the direct relationship between mining operations and mercury content in environment (Dołęgowska and Michalik 2019). Another study carried out to determine spatial distribution and risk assessment of Hg in Ganga Alluvial Plain, Lucknow region, India (Raju et al. 2019) revealed the probability of high health risk in 2/3 of the population residing in 58% of the area.

In our study, the arsenic concentration varies from 17 to 198 ppb in groundwater (Table 1). Concentrations of more than ten times the WHO limit are found at locations R3 (198 ppb), K1 (196ppb), V4 (128 ppb), RB (127 ppb), RK5 (117 ppb), A3 (111ppb) and A1

(110 ppb) (Fig. 4a). Locations A1, A3, K1 and R3 lie near Anpara TPP, Renusagar TPP, and Kakri coal mine. After the burning of coal in coal-based TPPs, arsenic enters into the atmosphere and contaminates water through leaching (Finkelman 2007; Baba et al. 2010). Earlier reports have established leaching from coal mines and TPPs as a major factor for water contamination (Baba et al. 2003; Agrawal et al. 2010, 2011; Tiwari et al. 2016). The high concentration of As is found in the vicinity of the coal mines or TPPs as clearly shown by the spatial distribution map prepared using IDW (Fig. 4a). However, there are certain locations such as RB, Rk5 and Rk4 that are away from mines or TPPS, yet have very high As concentration which may be because of the presence of other industries (Chemical and Aluminium) of Renukoot. There are certain locations such as V4, W1 having high As concentrations that lie in the vicinity of ash ponds (marked as grey colour in Fig. 4a). Wang et al. (1999) reported the contamination of groundwater because of the leaching of arsenic from ash. Harmful metals such as As can leach out from the storage of ash in these ash ponds and further contaminates groundwater. Similarly, high value of As (764.8 ppb) was observed in ground water of Hangjinhouqi country indicating the influence of mining and anthropogenic activity (Dong et al. 2019).

The concentration of arsenic varies from 12 to 209 ppb in surface water (Table 1). The highest concentration (209 ppb) is found in drain water at one location (V9) which is near to Vindhyachal TPP in Vindhya Nagar (Fig. 4b). Other high concentrations of arsenic in surface water are found at four locations viz. A7 (135ppb), V8 (66ppb), W7 (38ppb) and K6 (47 ppb). Interestingly, three samples namely A7, V8 and W7 lie in the vicinity of ash ponds. These ash ponds collect the ash generated from TPPs that contain arsenic in various forms. Ultimately, As deposited in these ash ponds

Table 2 Statistical analysis of the samples analysed for heavy metal (As, Hg, Pb and Cd) concentration in ppb; Heavy Metal Pollution Index (HPI), Contamination Index (CD) and Heavy Metal Evaluation Index (HEI)

Sr. no	Heavy metals and indices	Arsenic (ppb)	Mercury (ppb)	Lead (ppb)	Cadmium (ppb)	HPI[a]	CD[a]	HEI[a]
	Permissible limits (WHO 2011)	10	1	10	3	100	3	10
	Statistical parameter for ground water							
1	Minimum	17.00	4.00	4.00	2.00	2.16	0.46	1.46
2	Maximum	198.00	33.00	317.00	108.00	2941.09	77.83	81.83
3	Mean	78.81	10.67	79.16	34.40	901.85	23.34	26.89
4	Median	73.00	7.50	24.00	7.50	734.04	16.36	20.30
5	Standard deviation	49.07	7.86	83.14	38.59	708.07	20.64	20.91
6	Skewness	0.90	1.57	1.21	0.89	1.50	1.04	1.01
7	% of samples more than permissible limits	100.00	88.00	88.00	60.00	92.59	92.59	74.07
Sr. no	Heavy metals and indices	Arsenic (ppb)	Mercury (ppb)	Lead (ppb)	Cadmium (ppb)	HPI[c]	CD[c]	HEI[c]
	Permissible limits for effluent discharge (EPA 2002)	100	5	50	10	500	15	50
	Statistical parameter for surface water[b]							
1	Minimum	12.00	4.00	8.00	3.00	27.03	0.60	2.40
2	Maximum	209.00	22.00	122.00	40.00	1547.37	30.91	33.91
3	Mean	43.10	9.74	35.71	22.75	652.80	9.99	12.36
4	Median	31.00	10.00	28.00	24.00	578.26	8.58	10.58
5	Standard deviation	46.31	5.82	38.94	17.23	439.06	8.49	8.85
6	Skewness	2.91	0.96	2.39	−0.24	0.83	1.33	1.35
7	% of samples more than permissible limits	9.52	52.38	4.76	14.29	52.38	19.05	0.00

[a] The classification range for HPI, CD and HEI is based on Edet and Offiong 2002 and modified for this study

[b] The samples for surface water includes reservoir water, drain water, and pond water. Due to lack of permissible limits, we took the conservative approach and used effluent discharge limits given by EPA 2002 as that for surface water

[c] Since the regulations for Effluent discharge shows approximately 5 times the permissible limit of groundwater, hence the values of HPI, CD and HE for surface water have been kept 5 times those for groundwater

become a source which can further contaminate the aquatic environment through leaching. Earlier findings have reported high amounts of arsenic in both the surface and tube well water near coal based TPPs (Pandey et al. 2011). Comparatively lower concentrations are observed in all the samples of the reservoir dam: A6 (39 ppb), V12 (23 ppb), A5 (18 ppb), W4 (18ppb), V6 (16ppb), V7 (14ppb) and K9 (12 ppb). Due to the mixing with water of the reservoir, the As concentration is lower, still more than the WHO limit. Arsenic contamination of the environment including soil, surface water and groundwater in many parts of India has been related to mining activities (Agrawal et al. 2010, 2011; Masto et al. 2015; Sahoo et al. 2016; Tiwari et al. 2016). Recently, high level of arsenic (0.248 mg/L) was observed in surface water of Kütahya, western Turkey as the influence of mining activities (Şener and Karakuş 2017). With the exploitation of coal mines, burning of

coal in TPP, and dumping of ash in ash ponds will further irreversibly contaminate the environment.

The concentration of mercury varies from 5 to 33 ppb in groundwater samples exceeding the WHO limit of 1 ppb. High concentrations of Hg are observed at locations R4 (33 ppb), RK2 (29 ppb), K2 (19 ppb), V1 (16 ppb), R3 (16 PPB), V5 (15 ppb) and RK4 (14 ppb) (Table 1). Out of the samples; R4, R3, K2, K3 and V5 lie in the vicinity of Renusagar TPP, Kakri and Jayant coal mines as shown in (Fig. 4c). Similar observations are observed in Anpara region, where eight times higher concentration of Hg were found in groundwater (CSE 2011). Thus, the possibility of contamination from mine drainage as well as the burning of coal in TPPs cannot be ruled out. High concentration of mercury at location V1 (16 ppb) is due to the leaching of trace elements from ash as it is in the proximity of an ash pond (marked as grey colour in Fig. 4c). The
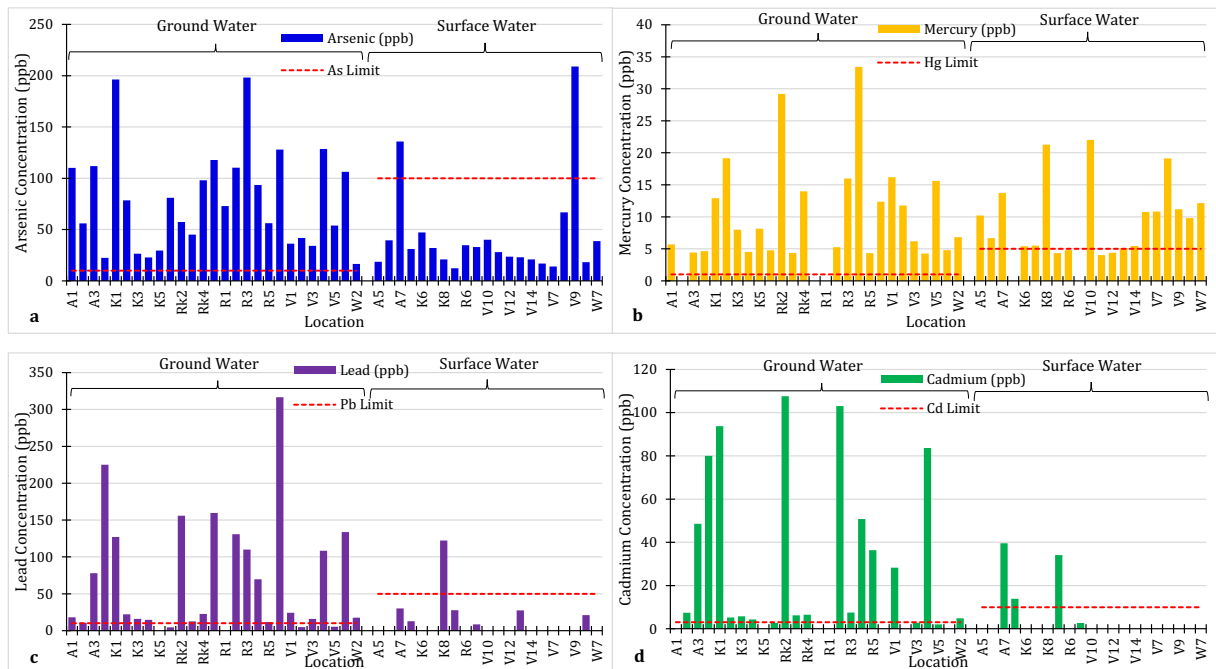
Fig. 3 Depiction of concentration of heavy metals in the groundwater and surface water of study area for **a** arsenic, **b** mercury, **c** lead and **d** cadmium. The dashed line in red colour shows the permissible limit for respective heavy metals as per WHO 2011 for groundwater and EPA 2002 for surface water that is conservatively considered as effluent discharge. (See the text and Tables 1 & 2 for more details)

groundwater gets contaminated because of leaching from ash ponds (Carlson and Adriano 1993; Agrawal et al. 2011). Thus, mercury contamination in the environment can be correlated with mining and combustion of coal in TPPs (Agrawal et al. 2010; Masto et al. 2015; Sahoo et al. 2016; Das et al. 2018).

In surface water, the concentration of mercury varies from 5 to 22 ppb (Table 1). High concentrations of Hg (between 10 and 20 times more than the WHO limit of 1 ppb) are observed at V10 (22 ppb), K8 (21 ppb), V8 (19 ppb) and A7 (13ppb) (Table 1). Out of these, K8 and V10 are samples of pond water that lie near Kakri and Khadia coal mines while locations A7 and V8 are situated near ash ponds (Fig. 4d). Similarly, high concentration of Hg (0.19 ppm) was observed in the ash pond near Bina/Kakri coal mine (Rai 2009). The release of Hg from ash ponds to surface as well as groundwater has been reported (Carlson and Adriano 1993; Twardowska et al. 2003; Agrawal et al. 2011). The water of the Rihand dam is also contaminated with high Hg concentration as observed in V8 (19 ppb), V7 (11 ppb) and V6 (11 ppb). Though the concentration is less because of the continuous influx of fresh water in the reservoir, it is still more than ten times the WHO limit. CSE has reported that the Dongiya drain that drains in the Rihand dam also has 10 ppb of Hg at the dam site (CSE 2011). Some other locations for drain water samples that were collected from Vindhya Nagar area (V9, V11, V13, V14) also have Hg concentration which can be related to the discharge from Vindhya Nagar TPP. Hence, this TPP seems to be the most probable reason for such high concentration of mercury in drain water. Thus, the operations of coal mines and TPPs' discharging drains, mine tailings, and ash in the form of a slurry, fly, and bottom ash that deposits high levels of mercury in the area cannot be overlooked.

Pollution evaluation indices

The indexing approach has emerged as an effective tool for the evaluation of heavy metal pollution in recent years. Many studies have used these methodologies to interpret the metal pollution in water resources (Yankey et al. 2013; Abou Zakhem and Hafez 2015; Milivojević et al. 2016; El- Hamid and Hegazy 2017).

In the present study, the HPI values for groundwater vary from 2.16 to 2941.09 with an average of 901.85 and a standard deviation of 694.83 (Table 2). For surface
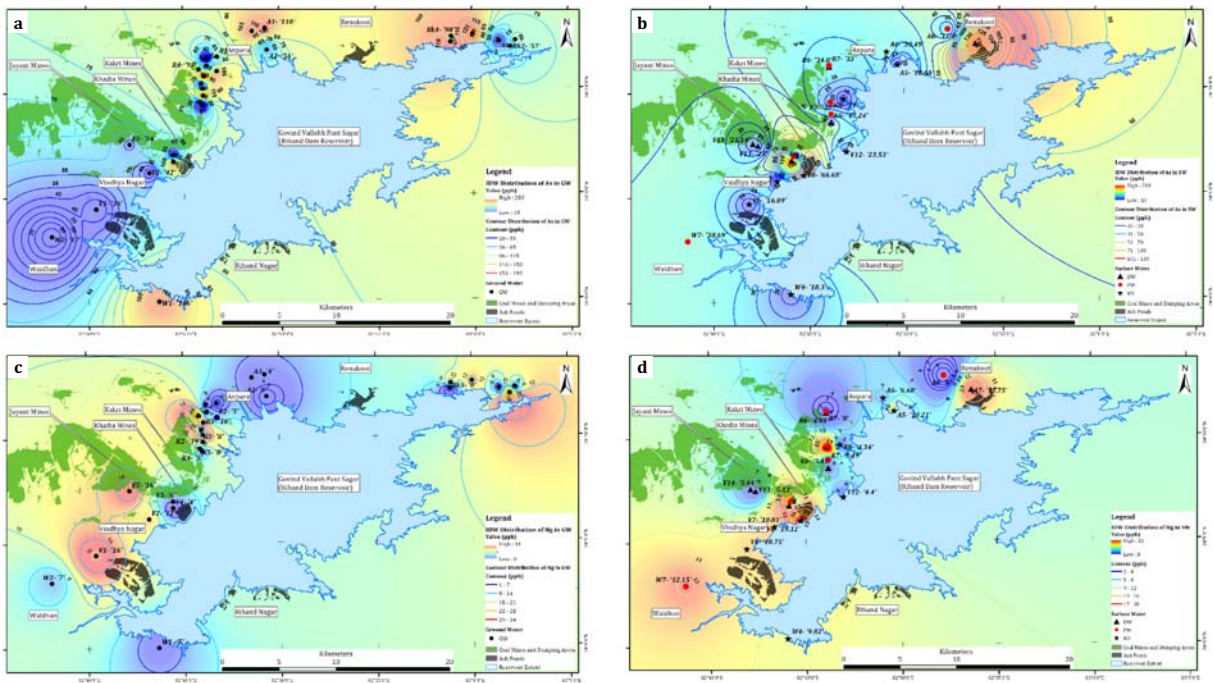
Fig. 4 Map showing spatial distribution of **a** As in groundwater, **b** As in surface water, **c** Hg in groundwater and **d** Hg in surface water. Groundwater sample locations are marked with black dot,

while sample locations marked with black triangle are for drain water, red dot for pond water, black star for Rihand dam and yellow dot for river water

water, HPI values range between 27.03 and 1547.37 and a mean of 652.80 with a standard deviation of 428.48 (Table 2). The highest HPI for groundwater is 2941.09 (Rk2), which is near Renukoot which has many industries surrounding it. Similar results are obtained in Thoothukudi District, Tamil Nadu, where different industries including TPPs are present, thus contaminating the groundwater with heavy metals leading to a maximum HPI value of 612 (Singaraja et al. 2015). 92% of the groundwater samples have HPI value greater than the critical value of 100 (Prasad and Bose 2001), indicating the unsuitability of groundwater for drinking. Recently, a study is carried out to determine the heavy metal pollution in ground water of Peenya Industrial Area in Bangalore (Shankar 2019) revealed very high HPI value (146.32) in ground water and a threat to public health. The regulations of heavy metal in effluent discharge shows approximately five times the permissible limit of groundwater, hence the values of HPI, CD and HE for surface water have been kept five times those for groundwater. In that respect, 52.38% of the surface water sample are exceeding the critical value of 500, indicating the unsuitability of surface water for irrigation purpose. Further, in surface water, the

maximum value of HPI is recorded in pond water K8 (1547.37) and V10 (1514.79) that is near Kakri and Khadia coal mines. Similarly, for drain water and reservoir dam, the maximum value of HPI reaches 1273.91 and 1317.55, respectively (Fig. 5). The HPI value recoded in Yamuna river of India was 176, which was above the critical value, such high value indicates the heavy metal pollution and influence of industrial activities (Rama Pal et al. 2017). Similar studies (Sisira Withanachchi et al. 2018) have been carried out to evaluate heavy metal pollution in Mashavera, Kazretula and Poladauri rivers. Mean HPI value is 80.676 in Uglješnica River, Serbia with the highest value recorded at one landfill site (Milivojević et al. 2016). In other study, the overall HPI value was found to be 350.14 in Damietta Nile branch water, indicating heavy metal pollution as a result of anthropogenic and industrial activities (Yasser El-Ameir 2017).

To estimate the extent of metal pollution, the CD is used as a reference and is calculated for different water types. For groundwater (hand pump), it ranges from 0.46 to 77.83 with an average of 23.34 and for surface water (drain, reservoir and pond), the CD value ranges from 0.60 to 30.91 with an average of 9.99 (Table 2).

The maximum CD values in surface water are 30.91 and 28.68 for pond and drain water, respectively. According to (Edet and Offiong 2002), the CD values can be classified into three categories: high (CD > 3), medium (CD, 1–3) and low (CD < 3). 92% of the ground and 19.05% of the surface water samples have CD values more than the critical value of 3 and 15 respectively (Table 2). In one study involving contamination of ground water in Saharanpur, Uttar Pradesh (India), CD value was seen to be 34.89, indicating the contamination of ground water with trace element (Kumar et al. 2019). Bhuiyan et al. (2010) observed similar findings where, CD value varies from 9 to 383 for surface water (mine drain water) in Dinajpur district of Bangladesh.

As mentioned earlier, heavy metal evaluation indices (HEI) is used for better evaluation and understanding of pollution indices (Edet and Offiong 2002). For surface water and groundwater samples, the range and average of HEI are 2.40–33.91, 12.36 and 1.46–81.83, 26.89, respectively. HEI value for surface water (mine drain water) ranges from 10 to 367 in Dinajpur district, Bangladesh (Bhuiyan et al. 2010). Because of spatial variability, the hydro-geochemical data are typically skewed i.e. the sets of data are not symmetric around the mean or median. Skewness and percentage deviation for both median and mean are shown in Table 2.

The values of HPI, CD and HEI that fall below their mean value, as indicated in Fig. 5, suggest relatively better water quality (Prasad and Bose 2001; Edet and Offiong 2002). From the value of all the three indices, it can be evaluated that both the surface water and groundwater are highly contaminated with heavy metals. Surface water is not suitable for irrigation and agricultural purposes as it will contaminate the soil with heavy metals, which can cause toxicity to agricultural produce (Mishra et al. 2014). Groundwater contaminated with heavy metal is not suitable for drinking and can cause several deadly diseases such as minimata, arsenicosis and itai-itai.

Land use/land cover

The spatial distributional pattern of land use/cover of the Singrauli study area for the years 2000, 2010 and 2016 is given in Fig. 6a, b, and c, respectively. Area-wise distribution of the land use/cover for the years 2000, 2010 and 2016 is mentioned in Table 3 and shown as the pie chart in Fig. 6d.

It is evident from Table 3 and Fig. 6, vegetation covered an area of 1145 km^2 in 2000 which is increased to 1466 km^2 in 2010 but decreased to 1258 km^2 in the next 6 years. Interestingly, the area under water body that was 424.38 km^2 (14.05%) in 2000, reduces to 308.11km^2 (10%) in the next 10 years (2010). Within 16 years, the area of the water body decreased by nearly 110 km^2. The area under fallow land covers 892 km^2 in
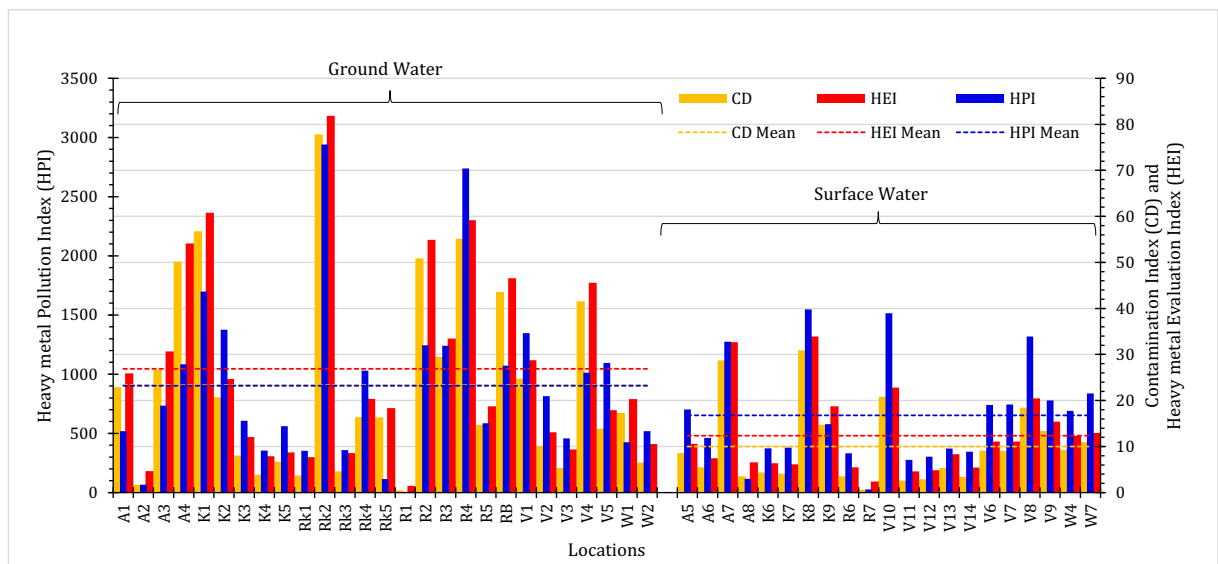

Fig. 5 Depiction of Contamination Index (CD); Heavy metal Evaluation Index (HEI and Heavy metal Pollution Index (HPI) in the ground and surface water of the study area. The dashed lines are the mean values for these indices (for more details, see Tables 1 and 2 and text)

2000 which is reduced to 608 km^2 in 2010. An overall decrease of 50.38 km^2 is observed from 2000 to 2016 in the fallow land area. An extensive change is observed in the ash pond area, which was 2.93 km^2 in 2000 and increases to 10.45 km^2 in 2010 showing a fast increasing trend. The continuous increase of dumping yard and overburden dump area is observed from 2000 to 2016. In 2000, overburden dumps occupied an area of 7.28 km^2 which increases to 13.59 km^2 in 2010 and further extends to 28.89 km^2 in 2016. Similarly, the mining area increases significantly from 2000 to 2016 with an overall increase of 17.79 km^2. Urban area was 29.18 km^2 in 2000 which increased to 72.24 km^2 in 2010 and 76.64 km^2 in 2016. The increase in mining area led to the migration and influx of people as a result of which urban area increased extensively. The reduction of the area of the land occupied by agriculture, bare land and water body is due to the expansion of coal mining activities, which has converted the area into overburden dumps, dump yards, mining areas, and fly ash ponds. The reduction of area under water body is possibly due to decline in annual rainfall, increase in withdrawal of water from Rihand reservoir for cooling the generators of TTPs and increased demand for water in coal washeries, water sprinkling on roads to stop dust generation on haul roads, dumpsites and in open cast mines.

It is interesting to note that the areas such as Shaktinagar, Anpara, Vindhynagar and Renukoot have expanded in terms of urbanization, industrialisation and extension of coal based TTPs. The upgradation and expansion of TPPs has led to increase in the size of ash ponds as visible in Fig. 6. These are the areas where heavy metal contamination have been observed. Specifically, the surface water of these regions is contaminated with As, Hg, Pb and Cd respectively (Fig. 4). In addition to these, there is a visible expansion of coal mining areas and their dumping yards as shown in Table 3 and Fig. 6, which has led to heavy metal contamination of ground water through leaching and contaminant transport.
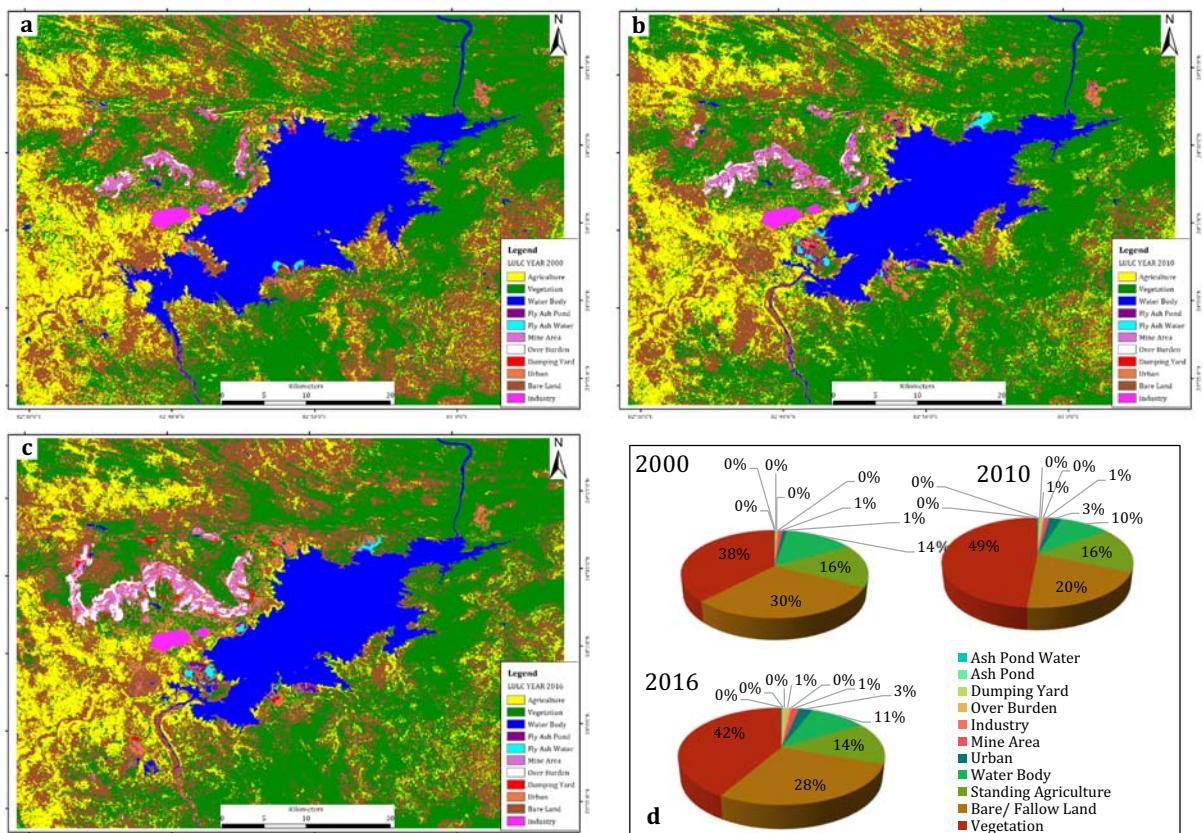

Fig. 6 Land use land cover (LULC) map of study area showing variation in different classes during **a** 2000, **b** 2010 and **c** 2016. The variation in different classes is shown in **d** pie chart for respective years

Table 3 Area wise distribution of land use/cover classes for the year 2000, 2010 and 2016

Sr. no	Land cover	2000		2010		2016		Area change (km^2)		
		Area (km^2)	% Area	Area (km^2)	% Area	Area (km^2)	% Area	2000–2010	2000–2016	2010–2016
1	Ash pond	2.93	0.10	10.45	0.35	6.92	0.23	7.52	3.99	− 3.53
2	Ash pond water	2.93	0.10	7.53	0.25	5.43	0.18	4.60	2.50	− 2.10
3	Bare/fallow land	892.25	29.53	608.11	20.13	841.87	27.86	− 284.15	− 50.38	233.76
4	Dumping yard	3.51	0.12	4.26	0.14	9.30	0.31	0.75	5.79	5.04
5	Industry	9.66	0.32	9.66	0.32	9.66	0.32	0.00	0.00	0.00
6	Mine area	22.57	0.75	28.97	0.96	40.36	1.34	6.40	17.78	11.39
7	Over burden	7.28	0.24	13.59	0.45	28.89	0.96	6.31	21.61	15.30
8	Standing agriculture	480.80	15.91	492.21	16.29	427.03	14.13	11.41	− 53.76	− 65.17
9	Urban	29.18	0.97	72.24	2.39	76.64	2.54	43.06	47.46	4.41
10	Vegetation	1145.80	37.92	1466.16	48.53	1258.78	41.66	320.36	112.98	− 207.38
11	Water body	424.38	14.05	308.11	10.20	316.40	10.47	− 116.27	− 107.98	8.29
	Total	3021.29	100.00	3021.29	100.00	3021.29	100.00	0.00	0.00	0.00

Areas such as Kakri mines and Jayant mines have higher contamination of Hg and As in the ground water (Fig. 4a, c). Thus, it is evident that the area where heavy metal contamination is observed are situated near the coal mines, coal-based TPPs and their respective ash ponds. A study carried out to determine the Spatio-temporal dynamics of LULC change in Singrauli area (Kumari and Sarma 2017, Kumar et al. 2019) revealed an increase in the wasteland and marshy area and a decline in the forest area. Similarly, LULC studies carried out during 2010–2015 in the same study area (Ahmad and Goparaju 2017) exhibited an increase of 573 ha of mining land area. Hence, the environmental degradation could be strongly attributed to anthropogenic activities in this region that needs to be critically assessed and studied in detail.

Conclusion

Both the ground and surface water samples are contaminated with heavy metals such as As, Hg, Pb and Cd at alarming levels, as concentrations of them were found to be above (WHO) permissible limit in most of the samples. Similarly, HPI, HEI and CD values indicate high heavy metal pollution and contamination in the water bodies of the Singrauli area. Almost all the groundwater samples are contaminated with Hg and As, which make it unsuitable for drinking and domestic purposes. Interpretation of spatial distribution of heavy metals Hg and

As shows that most of the contaminated samples lie in the vicinity of thermal power plants, mining area and ash ponds. The ash ponds act as a source for such contamination which leaches to groundwater and contaminates the nearby hand pumps. Major LULC changes have been recorded that include a reduction in the water bodies and agricultural land while showing increases in the mining area, fly ash ponds and dump yards. During these 16 years, there is a fourfold increase in the overburden, a threefold increase in dumping yard, 2.5 times increase in urban areas and a twofold increase in the mining area.

From the above changes, it can be interpreted that both the mining and industrial activities have greatly impacted the environment and the hydrosphere of the region. With the increasing population, both the scarcity of water and its contamination are prevalent in this study area thus affecting the population health. Hence, there is a need for proper regulation, monitoring and treatment of the water resources. The result of this study shall be considered with utmost priorities by the concerned water resource authority for abatement of ground and surface water pollution in this area. Hence, further pollution must be prevented by proper management practices. There should be strict guidelines and penalty for discharge of untreated wastewater into water bodies. Such studies can be considered as a better platform and suitable mode for assessment of water quality. Further, the study has relevance in making action plans for reducing the heavy metal influx into the groundwater.

References

Abou Zakhem, B., & Hafez, R. (2015). Heavy metal pollution index for groundwater quality assessment in Damascus Oasis, Syria. *Environment and Earth Science, 73*, 6591–6600.

Agrawal, P., Mittal, A., Prakash, R., Kumar, M., Singh, T. B., & Tripathi, S. K. (2010). Assessment of contamination of soil due to heavy metals around coal fired thermal power plants at Singrauli region of India. *Bulletin of Environmental Contamination Toxicololgy, 85*, 219–223.

Agrawal, P., Mittal, A., Prakash, R., Kumar, M., & Tripathi, S. K. (2011). Contamination of drinking water due to coal-based thermal power plants in India. *Environment Forensics., 12*, 92–97.

Ahmad, F., & Goparaju, L. (2017). Spatio-temporal dynamics of mines in Singrauli, India: an analysis using geospatial technology. *Journal of Geomatics, 11*, 53–59.

Baba, A., Kaya, A., & Birsoy, Y. K. (2003). The effect of Yatagan thermal power plant (Mugla, Turkey) on the quality of surface and groundwaters. *Water, Air, and Soil Pollution, 149*, 93–111.

Baba, A., Gurdal, G., & Sengunalp, F. (2010). Leaching characteristics of fly ash from fluidized bed combustion thermal power plant: case study: Çan (Çanakkale-Turkey). *Fuel Process Technologgy, 91*, 1073–1080.

Backman, B., Bodis, D., Lahermo, P., & Rapant, S. (1997). Application of a groundwater contamination index in Finland and Slovakia. *Environmental Geology, 36*, 55–64.

Bhuiyan, M. A. H., Parvez, L., Islam, M. A., Dampare, S. B., & Suzuki, S. (2010). Heavy metal pollution of coal mine-affected agricultural soils in the northern part of Bangladesh. *Journal of Hazardous Material, 173*, 384–392.

BIS (Bureau of Indian Standards) (2012) *Drinking water specification*. New Delhi: Bureau of Indian standards.

Brindha, K., Neena Vaman, K. V., Srinivasan, K., Sathis Babu, M., & Elango, L. (2014). Identification of surface water-groundwater interaction by hydrogeochemical indicators and assessing its suitability for drinking and irrigational purposes in Chennai, Southern India. *Applied Water Science, 4*, 159–174.

Carlson, C. L., & Adriano, D. C. (1993). Environmental impacts of coal combustion residues. *Journal of Environmental Quality, 22*(2), 227–247.

CGWB (2013) Central Ground Water Board, Ministry of Water Resources, Government of India. Ground Water Brochure, Singrauli district, Uttar Pradesh, India.

Chakraborti, D., Rahman, M. M., Das, B., Nayak, B., Pal, A., Sengupta, M. K., Hossain, M. A., Ahamed, S., Sahu, M., Saha, K. C., Mukherjee, S. C., Pati, S., Dutta, R. N., & Quamruzzaman, Q. (2013). Groundwater arsenic contamination in Ganga-Meghna-Brahmaputra plain, its health effects and an approach for mitigation. *Environment Earth Science, 70*, 1993–2008.

Chowdhury, S., Mazumder, M. J., Al-Attas, O., & Husain, T. (2016). Heavy metals in drinking water: occurrences, implications, and future needs in developing countries. *Science of Total Environment, 569*, 476–488.

CSE. (2011). *Mercury pollution in Sonbhadra district of Uttar Pradesh and its health impacts* (p. 110062). Centre for Science and Environment. Tughlakabad Institutional Area, New Delhi.

Das, A., Patel, S. S., Kumar, R., Krishna, K. V. S. S., Dutta, S., Saha, M. C., Sengupta, S., & Guha, D. (2018). Geochemical sources of metal contamination in a coal mining area in Chhattisgarh, India using lead isotopic ratios. *Chemosphere, 197*, 152–164.

Dimyati, M., Mizuno, K., Kobayashi, S., & Kitamura, T. (1996). An analysis of land use/cover change in Indonesia. *International Jornal of Remote Sensing, 17*(5), 931–944.

Dołęgowska, S., & Michalik, A. (2019). The use of a geostatistical model supported by multivariate analysis to assess the spatial distribution of mercury in soils from historical mining areas: Karczówka Mt., Miedzianka Mt., and Rudki (south-central Poland). *Environmental monitoring and assessment, 191*(5), 302.

Dong, Y. H., Li, J. L., & Ma, T. (2019). Hydrochemical characteristics and the genesis of high arsenic groundwater in the ecotone between polymetallic sulfide mining area and irrigated agricultural area. In Environmental arsenic in a changing world: proceedings of the 7th International Congress and Exhibition on Arsenic in the Environment (AS 2018), July 1-6, 2018, Beijing, PR China (p. 161). CRC Press.

Dubey, C. S., Mishra, B. K., Shukla, D. P., Singh, R. P., Tajbakhsh, M., & Sakhare, P. (2012). Anthropogenic arsenic menace in Delhi Yamuna flood plains. *Environment Earth Science, 65*, 131–139.

Dwivedi, A. K., & Vankar, P. S. (2014). Source identification study of heavy metal contamination in the industrial hub of Unnao, India. *Environment Monitoring Assessment, 186*(6), 3531–3539.

Edet, A. E., & Offiong, O. E. (2002). Evaluation of water quality pollution indices for heavy metal contamination monitoring. A study case from Akpabuyo-Odukpani area, Lower Cross River basin (South-Eastern Nigeria). *Geo Journal, 57*(4), 295–304.

El- Hamid, H. T. A., & Hegazy, T. A. (2017). Evaluation of water quality pollution indices for groundwater resources of New Damietta, Egypt. *MOJ Ecology Environmental Science, 2*(6), 00045.

El-Ameir, Y. A. (2017). Evaluation of heavy metal pollution in Damietta branch of Nile River, Egypt using metal indices and phyto-accumulators. *Journal of Environmental Sciences, 46*, 89–102.

Environmental Protection Act, (2002). *Standards for Effluent Discharge Regulations. General Notice No. 44. of 2003*. Available from: http://faolex.fao.org/docs/texts/mat52519.doc. Accessed 3 Sept 2020.

Finkelman, R. B. (2007). Health impacts of coal: facts and fallacies. *AMBIO - A J Human Environment, 36*, 103–106.

Förstner, U., & Wittmann, G. T. (2012). *Metal pollution in the aquatic environment*. Springer Science & Business Media.

Fytianos, K., Tsaniklidi, B., & Voudrias, E. (1998). Leachability of heavy metals in Greek fly ash from coal combustion. *Environment International, 24*, 477–486.

Ghosh, M., Pal, D. K., & Santra, S. C. (2019). Spatial mapping and modeling of arsenic contamination of groundwater and risk assessment through geospatial interpolation technique. *Environment, Development and Sustainability*, 1–20.

Giri, S., & Singh, A. K. (2014). Assessment of surface water quality using heavy metal pollution index in Subarnarekha River, India. *Water Quality Exposure Health, 5*, 173–182.

Gowda, N. K. S., Malathi, V., Jash, S., & Roy, K. S. (2003). Status of pollutants and trace elements in water, soil, vegetation and dairy animals in industrial area of Bangalore. *Indian Journal of Dairy Science, 56*(2), 86–90.

Raju, N. J., Dey, S., & Das, K. (2009). Fluoride contamination in groundwaters of Sonbhadra District, Uttar Pradesh, India. *Current Science, 96*, 979–985.

Kalita, S., Sarma, H. P., & Devi, A. (2019). Sediment characterisation and spatial distribution of heavy metals in the sediment of a tropical freshwater wetland of Indo-Burmese province. *Environmental Pollution, 250*, 969–980.

Khan, I., Javed, A., & Khurshid, S. (2013). Physico-chemical analysis of surface and groundwater around Singrauli Coal Field, District Singrauli, Madhya Pradesh, India. *Environment Earth Science, 68*, 1849–1861.

Kim, A. G., & Kazonich, G. (1999). Mass release of trace elements from coal combustion by-products. In *International Ash Utilization Symposium*. Lexington, KY: Centre for Applied Energy Research, University of Kentucky.

Kumar, A., & Ahmad, T. (2007). Geochemistry of mafic dykes in part of Chotanagpur gneissic complex: petrogenetic and tectonic implications. *Geochemistry Journal, 41*, 173–186.

Kumar, M., Nagdev, R., Tripathi, R., Singh, V. B., Ranjan, P., Soheb, M., & Ramanathan, A. L. (2019). Geospatial and multivariate analysis of trace metals in tubewell water using for drinking purpose in the upper Gangetic basin, India: heavy metal pollution index. *Groundwater for Sustainable Development, 8*, 122–133.

Kumari, M., & Sarma, K. (2017). Changing trends of land surface temperature in relation to land use/cover around thermal power plant in Singrauli district, Madhya Pradesh, India. *Spatial Information Research, 25*(6), 769–777.

Li, F., Li, X., Hou, L., & Shao, A. (2018). Impact of the coal mining on the spatial distribution of potentially toxic metals in farmland tillage soil. *Scientific Reports, 8*, 1–10.

Lü, J., Jiao, W. B., Qiu, H. Y., Chen, B., Huang, X. X., & Kang, B. (2018). Origin and spatial distribution of heavy metals and carcinogenic risk assessment in mining areas at You'xi county Southeast China. *Geoderma, 310*, 99–106.

Machiwal, D., & Jha, M. K. (2014). Characterizing rainfall-groundwater dynamics in a hard-rock aquifer system using time series, geographic information system and geostatistical modelling. *Hydrological Processes, 28*, 2824–2843.

Masto, R. E., Sheik, S., Nehru, G., Selvi, V. A., George, J., & Ram, L. C. (2015). Assessment of environmental soil quality around Sonepur Bazari mine of Raniganj coalfield, India. *Solid Earth., 6*, 811–821.

Mehta, P. S., (2002). The Indian mining sector: effects on the environment and FDI inflows. Paper presented in: CCNM global forum on international investment, conference on foreign direct investment and the environment - lessons to be learned from the mining sector", 7–8 February, OECD headquarters, Paris, France.

Milivojević, J., Krstić, D., Šmit, B., & Djekić, V. (2016). Assessment of heavy metal contamination and calculation of its pollution index for Uglješnica River, Serbia. *Bulletin of Environmental Contamination and Toxicology, 97*(5), 737–742.

Mishra, B. K., Dubey, C. S., Shukla, D. P., Bhattacharya, P., & Usham, A. L. (2014). Concentration of arsenic by selected vegetables cultivated in the Yamuna flood plains (YFP) of Delhi, India. *Environment Earth Science, 72*(9), 3281–3291.

Pandey, V. C., Singh, J. S., Singh, R. P., Singh, N., & Yunus, M. (2011). Arsenic hazards in coal fly ash and its fate in Indian scenario. *Resources, Conservation and Recycling, 55*(9–10), 819–835.

Prasad, B., & Bose, J. M. (2001). Evaluation of heavy metal pollution index for surface and spring water near a limestone mining area of the lower Himalayas. *Environmental Geology, 41*, 183–188.

Prasad, A. K., Singh, R. P., & Kafatos, M. (2012). Influence of coal-based thermal power plants on the spatial-temporal variability of tropospheric NO2 column over India. *Environment Monitoring Assessment, 184*, 1891–1907.

Qasemi, M., Shams, M., Sajjadi, S. A., Farhang, M., Erfanpoor, S., Yousefi, M., Zarei, A., & Afsharnia, M. (2019). Cadmium in groundwater consumed in the rural areas of Gonabad and Bajestan, Iran: occurrence and health risk assessment. *Biological Trace Element Research, 192*(2), 106–115.

Rai, P. K. (2008). Mercury pollution from a chloralkali source in a tropical Lake and its biomagnification in aquatic biota: Link between chemical pollution, biomarkers, and human health concern. *Human and Ecological Risk Assessment, 14*(6), 1318–1329.

Rai, P. K. (2009). Heavy metals in water, sediments and wetland plants in an aquatic ecosystem of tropical industrial region, India. *Environmental Monitoring and Assessment, 158*(1–4), 433–457.

Raju, A., Singh, A., Srivastava, N., Singh, S., Jigyasu, D. K., & Singh, M. (2019). Mapping human health risk by geostatistical method: a case study of mercury in drinking groundwater resource of the central ganga alluvial plain, northern India. *Environmental Monitoring and Assessment, 191*(2), 298.

Rama Pal, D. R. K., Dubey, S. K., & Singh, A. K. (2017). Assessment of heavy metal pollution through index analysis for Yamuna water in Agra Region, India. *International Journal of Current Microbiology and Applied Sciences, 6*, 1491–1498.

Rashid, A., Khan, S., Ayub, M., Sardar, T., Jehan, S., Zahir, S., Khan, M. S., Muhammad, J., Khan, R., Ali, A., & Ullah, H. (2019). Mapping human health risk from exposure to potential toxic metal contamination in groundwater of Lower Dir, Pakistan: application of multivariate and geographical information system. *Chemosphere, 225*, 785–795.

Rawat, J., & Kumar, M. (2015). Monitoring land use/cover change using remote sensing and GIS techniques: a case study of Hawalbagh block, district Almora, Uttarakhand, India.

Egyptian Journal of Remote Sensing and Space Science, 18(1), 77–84.

Sahoo, P. K., Kim, K., Powell, M. A., & Equeenuddin, S. M. (2016). Recovery of metals and other beneficial products from coal fly ash: a sustainable approach for fly ash management. *International Journal of Coal Science & Technology, 3*(3), 267–283.

Sahu, R., Saxena, P., Johnson, S., Mathur, H. B., & Agarwal, H. C. (2014). Mercury pollution in the Sonbhadra district of Uttar Pradesh, India, and its health impacts. *Toxicological & Environmental Chemistry, 96*(8), 1272–1283.

Sankararamakrishnan, N., Chauhan, D., Nickson, R. T., Tripathi, R. M., & Iyengar, L. (2008). Evaluation of two commercial field test kits used for screening of groundwater for arsenic in northern India. *Science of the Total Environment, 401*(1–3), 162–167.

Selvam, S., Venkatramanan, S., & Singaraja, C. (2015). A GIS-based assessment of water quality pollution indices for heavy metal contamination in Tuticorin corporation, Tamilnadu, India. *Arabian Journal of Geosciences, 8*(12), 10611–10623.

Şener, Ş., & Karakuş, M. (2017). Investigating water quality and arsenic contamination in drinking water resources in the Tavşanlı District (Kütahya, Western Turkey). *Environmental Earth Sciences, 76*(21), 750.

Shankar, B. S. (2019). A critical assay of heavy metal pollution index for the groundwaters of Peenya Industrial Area, Bangalore, India. *Environmental Monitoring and Assessment, 191*(5), 289.

Sharma, R. K., Agrawal, M., & Marshall, F. (2007). Heavy metal contamination of soil and vegetables in suburban areas of Varanasi, India. *Ecotoxicology and Environment Safety, 66*(2), 258–266.

Shukla, D. P., Dubey, C. S., Singh, N. P., Tajbakhsh, M., & Chaudhry, M. (2010). Sources and controls of arsenic contamination in groundwater of Rajnandgaon and Kanker District, Chattisgarh Central India. *Journal of Hydroog, 395*, 49–66.

Simeonov, V., Stratis, J. A., Samara, C., Zachariadis, G., Voutsa, D., Anthemidis, A., Sofoniou, M., & Kouimtzis, T. (2003). Assessment of the surface water quality in northern Greece. *Water Resources, 37*(17), 4119–4124.

Singaraja, C., Chidambaram, S., Srinivasamoorthy, K., Anandhan, P., & Selvam, S. (2015). A study on assessment of credible sources of heavy metal pollution vulnerability in groundwater of Thoothukudi districts, Tamilnadu, India. *Water Quality, Exposure and Health, 7*(4), 459–467.

Singh, U. K., & Kumar, B. (2017). Pathways of heavy metals contamination and associated human health risk in Ajay River basin, India. *Chemosphere, 174*, 183–199.

Singh, C. K., & Srivastava, V. (2011). Morphotectonics of the area around Renukoot, district Sonbhadra, UP using remote sensing and GIS techniques. *Journal of the Indian Society of Remote Sensing, 39*(2), 235–240.

Singh, K. P., Mohan, D., Singh, V. K., & Malik, A. (2005). Studies on distribution and fractionation of heavy metals in Gomti river sediments—a tributary of the Ganges, India. *Journal of Hydrology, 312*(1–4), 14–27.

Singh, A. P., Ghosh, S. K., & Sharma, P. (2007). Water quality management of a stretch of river Yamuna: an interactive fuzzy multi-objective approach. *Water Resource Management, 21*, 515–532.

Singh, P. K., Singh, M. P., Volkmann, N., Naik, A. S., & Börner, K. (2014). Petrological characteristics of lower Gondwana coal from Singrauli coalfield, Madhya Pradesh, India. *International Journal of Oil, Gas and Coal Technology, 8*(2), 194–220.

Singh, R., Kumar, S., & Singh, A. (2018). Elevated black carbon concentrations and atmospheric pollution around Singrauli coal-fired thermal power plants (India) using ground and satellite data. *International Journal of Environmental Research and Public Health, 15*(11), 2472.

Sisira Withanachchi, S., Ghambashidze, G., Kunchulia, I., Urushadze, T., & Ploeger, A. (2018). Water quality in surface water: a preliminary assessment of heavy metal contamination of the Mashavera River, Georgia. *International Journal of Environmental Research and Public Health, 15*, 621.

Soni, R., & Shukla, D. P. (2018). Synthesis of Fly ash based zeolite-reduced graphene oxide composite and its evaluation as an adsorbent for arsenic removal. *Chemosphere., 219*, 504–509.

Swash, P. (2003). *Field evaluation of the Wagtech Arsenator.* London: Royal School of Mines, Imperial College.

Tiwari, A. K., Singh, P. K., & Mahato, M. K. (2014). GIS-based evaluation of water quality index of ground water resources in West Bokaro Coalfield, India. *Current World Environment, 9*(3), 843.

Tiwari, A. K., Singh, P. K., Singh, A. K., & De Maio, M. (2016). Estimation of heavy metal contamination in groundwater and development of a heavy metal pollution index by using GIS technique. *Bulletin of Environment Contamination and Toxicology, 96*(4), 508–515.

Torregroza-Espinosa, A. C., Martínez-Mera, E., Castañeda-Valbuena, D., González-Márquez, L. C., & Torres-Bejarano, F. (2018). Contamination level and spatial distribution of heavy metals in water and sediments of El Guajaro reservoir, Colombia. *Bulletin of Environmental Contamination and Toxicology, 101*(1), 61–67.

Twardowska, I., Tripathy, P. S. M., Singh, G., & Kyziol, J. (2003). *Trace elements and their mobility in coal ash/fly ash from Indian power plants in view of its disposal and use in agriculture* (pp. 25–24). Boston, MA: Chemistry of Trace Elements in Fly Ash. Springer.

United Nations/World Water Assessment Programme UN/WWAP (2003) UN World Water Development Rep. Water for People, Water for Life, United Nations Educational, Scientific and Cultural Organization and Berghahn Books, Paris.

Usham, A. L., Dubey, C. S., Shukla, D. P., Mishra, B. K., & Bhartiya, G. P. (2018). Sources of fluoride contamination in Singrauli with special reference to Rihand reservoir and its surrounding. *Journal of the Geological Society of India, 91*(4), 441–448.

Wang, Y., Ren, D., & Zhao, F. (1999). Comparative leaching experiments for trace elements in raw coal, laboratory ash, fly ash and bottom ash. *International Journal of Coal Geology, 40*(2–3), 103–108.

WHO. (2011). *Guidelines for drinking-water quality* (4th ed.). Geneva: World Health Organization.

Yadav, S., Upadhyay, S., Tripathi, S. K., & Prakash, R. (2017). Heavy metal pollution and health hazards around Singrauli region India. *IJAR, 3*(5), 05–08.

Yankey, R. K., Fianko, J. R., Osae, S., Ahialey, E. K., Duncan, A. E., Essuman, D. K., & Bentum, J. K. (2013). Evaluation of heavy metal pollution index of groundwater in the Tarkwa mining area, Ghana. *Elixir Pollution, 54*, 12663–12667.

Yano, Y., Ito, K., Kodama, A., Shiomori, K., Tomomatsu, S., Sezaki, M., & Yokota, H. (2012). Arsenic polluted groundwater and its countermeasures in the Middle Basin of the Ganges, Uttar r, Indjria. *Journal of Environment Protection, 3*, 856–862.

Zhang, Y., Chu, C., Li, T., Xu, S., Liu, L., & Ju, M. (2017). A water quality management strategy for regionally protected water through health risk assessment and spatial distribution of heavy metal pollution in 3 marine reserves. *Science of the Total Environment, 599*, 721–731.